2019 IEEE Intelligent Transportation Systems Conference (ITSC)
Auckland, NZ, October 27-30, 2019

Lane Change Maneuver based on Bezier Curve providing Comfort Experience for Autonomous Vehicle Users

Il Bae[1], Jin Hyo Kim[2], Jaeyoung Moon[1] and Shiho Kim[1], *Member, IEEE*

***Abstract*— Comfort driving has emerged as an important topic in the autonomous car research field. This study focuses on lane change maneuvering (LCM) of autonomous vehicles to provide a comfortable driving experience for passengers. For this purpose, we propose an LCM algorithm for determining a desired trajectory by evaluating the allowable lateral acceleration value obtained from Bezier curves at a local path planning stage for comfortable and smooth motion of the vehicle. The performance of the proposed LCM algorithm was verified through computer simulations and real driving tests.**

I. Introduction

Autonomous self-driving vehicles are expected to achieve an outstanding effect in reducing traffic accidents as well as in improving traffic and fuel efficiency. Recently, ride quality has emerged as an important issue in the autonomous driving research field [1-6]. For the autonomous vehicles at level-3 or higher [7], a driver is no longer needed to control the vehicle actuators nor pay attention to obtain the preview information. In other words, a driver who controls an autonomous driving vehicle becomes a passenger. This implies that an automated vehicle has the potential to cause motion sickness to drivers or passengers.

Comfort driving is a term used to describe a person's subjective perception of a vehicle ride. It is difficult to define what constitutes a good ride quality because comfort is related to a human mentality, however, several studies have reported that vehicle acceleration affects the quality of a ride [1-4]. Good ride quality is associated with passenger comfort and reduced risk of motion sickness. Motion sickness mainly results from a conflict between the human body's vestibular and visual sensory systems [5-6]. The smaller the difference between these systems, the more comfortable the ride. A high value of acceleration can cause discomfort even for short rides.

Generally, passengers experience less motion sickness when they take a train than a bus, because the frequency of change in speed, which is the magnitude of acceleration, is relatively lower. In case of trains, they manage the desired velocity regarding the radius of the route for a smooth transition [8-9], thus, leading to lower difference in dynamic motion between the vision and vestibular systems of the human body, thereby making the ride more comfortable. Therefore, to enhance the driving experience, the above factors need to be considered and smooth driving strategies are required [21-22]. Careful control of the acceleration, braking, and steering actions of the vehicle can improve the comfort of the passengers. In case of public transportation (i.e, train), the speed and acceleration profile are strictly managed based on the common criterion of "longitudinal and lateral accelerations" within 0.9 m/s^2 [1-2, 4, 8-9]. This criterion can also be applied to autonomous driving vehicles.

In particular, lateral acceleration of vehicles typically arises during swift lane changes or at curves. The main goal of this study is to provide a comfortable driving experience for autonomous vehicle passengers during lane change maneuvering (LCM). There are various techniques used to effect lane change for unmanned vehicles, but Bezier curves have widely been used to generate routes for LCM. Choi [10] proposed path planning algorithms for UGV based on a 3rd-order Bezier curve that generates a reference trajectory to satisfy the corridor constraints. Han [11] developed a path planner with a collision-avoidance system based on a 4th-order Bezier curve that takes into account the sum of all path lengths subjected to distances between the mobile robots. Chen [12] developed a lane change algorithm based on Bezier curves considering the non-holonomic constraints of vehicle steering with a yaw rate parameter. Kawabata [13] proposed Bezier curve generation including 3-dimensional cases based on a constrained optimization solver.

Conventional methods based on Bezier curves have insufficient capability to provide driving comfort in the case of a lane change maneuver because prior works focus on precise robotic control to follow a given path. However, the proposed LCM algorithm can provide comfortable experience during lane changes because it can bound the lateral acceleration value as a control parameter in spite of various speed conditions. We propose an LCM algorithm based on evaluating the expected maximum lateral acceleration using the curvature of a Bezier curve and following the generated trajectory. This method was implemented and performed by a car simulator and a real test with an autonomous vehicle. The test results validate the feasibility of the proposed LCM algorithm.

The remainder of this paper is organized as follows. In Section II, we explain the vehicle model and controller. Section III describes the LCM algorithm based on the quantic Bezier curve. Computer simulations and experimental results are presented in Sections IV and V while Section VI serves as the conclusion.

II. Lateral and Longitudinal Controller

A. Lateral Vehicle Model with State Feedback Control

An integrated longitudinal and lateral controller is required to track the planned trajectory with desired speed for various driving states of an autonomous vehicle [14, 20].

[1] Il Bae, Jaeyoung Moon and Shiho Kim are with the Seamless Transportation Lab, School of Integrated Technology, and Yonsei Institute of Convergence Technology, Yonsei University, Incheon, South Korea. (e-mail: kakao@yonsei.ac.kr; ekuno90@yonsei.ac.kr; shiho@yonsei.ac.kr)
[2] Jin Hyo Kim is with Robotics Research Lab., Dogugonggan Co., Ltd., Seoul, South Korea. (e-mail: ceo@dogu.xyz)

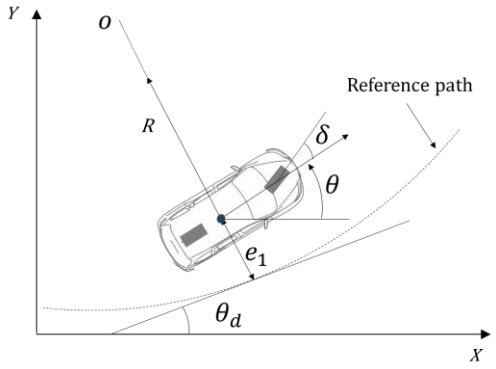

Figure 1. Geometric relationship between the lateral control parameters.

The vehicle's lateral kinematics is modeled based on a linear bicycle model. This is achieved by lumping the right and left wheels together at the centers of the front and rear axles. The motion of the vehicle is assumed to be in planar geometry in the Cartesian coordinate system. Fig. 1 shows the geometric relationship of the proposed steering control parameters. This model assumes that only the front steering angle is controllable, and the rear steering could be set to zero.

If the vehicle travels at a constant speed on a road with a constant radius, then [14, 15],

$$\dot{\theta}_d = V_x/R = V_x k \tag{1}$$

where $\dot{\theta}_d$ denotes the desired yaw rate of the vehicle. V_x is the longitudinal speed and $R(=1/\mathrm{k})$ is the radius of the path.

$x = [e_1, \dot{e}_1, e_2, \dot{e}_2]^{\mathrm{T}}$, where e_1 and e_2 are the distances of the c.g. of the vehicle from the reference path and the orientation error with respect to the road, respectively. The dynamics of vehicle is presented as in [15],

$$\dot{x} = Ax + B_1 u + B_2 \dot{\theta}_{des} \tag{2}$$

$$A = \begin{bmatrix} 0 & 1 & 0 & 0 \\ 0 & -\frac{2C_{af}+2C_{ar}}{mV_x} & \frac{2C_{af}+2C_{ar}}{m} & \frac{-2C_{af}+2C_{ar}l_r}{mV_x} \\ 0 & 0 & 0 & 1 \\ 0 & -\frac{2C_{af}l_f-2C_{ar}l_r}{I_zV_x} & -\frac{2C_{af}l_f+2C_{ar}l_r}{I_z} & -\frac{2C_{af}l_f^2+2C_{ar}l_r^2}{I_zV_x} \end{bmatrix}$$

$$B_1 = \begin{bmatrix} 0 \\ \frac{2C_{af}}{m} \\ 0 \\ \frac{2C_{af}l_f}{I_z} \end{bmatrix}, B_2 = \begin{bmatrix} 0 \\ -\frac{2C_{af}l_f-2C_{ar}l_r}{mV_x} - V_x \\ 0 \\ -\frac{2C_{af}l_f^2+2C_{ar}l_r^2}{I_zV_x} \end{bmatrix}$$

The matrix A has two eigenvalues at the origin and is unstable, hence, this system must be stabilized by feedback. State feedback is utilized by commanding the input vector, u, as shown in Fig. 2. Consider a proportional input with a feed-forward term, $u = -Kx + \delta$, then, the closed-loop system is given by

$$\dot{x} = [A - B_1 K]x + B_1\delta + B_2\dot{\theta}_{des} \tag{3}$$

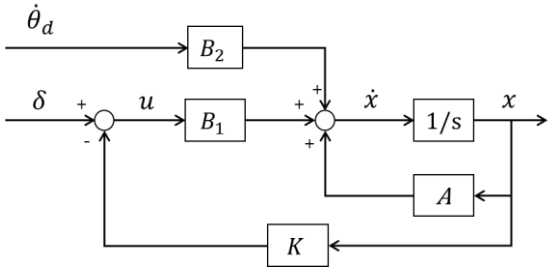

Figure 2. Block diagram of the state feedback steering controller.

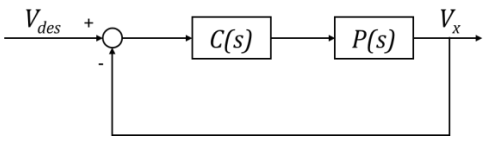

Figure 3. Vehicle model, P(s) with PD controller, C(s) for cruise control.

K is chosen as [0.3 0.03 2 0.01]. Due to the $B_1\delta + B_2\dot{\theta}_{des}$ term in Eq. (2), the path tracking error will not converge to zero. Since the vehicle is a rigid body, both its lateral position error, e_1, and its angular error e_2, cannot converge to zero simultaneously. If the lateral position error is zero, then the heading angle error can be zero in a case where only the slip angle at the rear wheel of the vehicle is the same. However, the distance error, e_1 can be made zero through appropriate steering input. The steady-state steering angle for zero distance error is given by [16]

$$\delta = tan^{-1}\left\{\frac{l_f+l_r}{l_r}\cdot tan(sin^{-1}(l_r\cdot k_v))\right\} \tag{3}$$

where δ denotes the steady state steering angle for zero distance error derived from the location of center of gravity regarding the body slip angle of the vehicle. l_f (l_r) denotes the length of the center of gravity of the vehicle to the front axle (rear axle) and k_v represents the instantaneous curvature of the vehicle.

B. Longitudinal Vehicle Model for Cruise

A typical PD control algorithm is used for the upper level controller for maintaining a constant speed for the vehicle using feedback. The PD controller of the transfer function is given by [15]

$$C(s) = K_P + K_D s \tag{4}$$

The plant model for the controller is the transfer function between the desired acceleration and the actual vehicle speed and is given by

$$P(s) = \frac{1}{ts^2+s} \tag{5}$$

Then, the closed-loop transfer function can be expressed as

$$\frac{V_{des}}{V_x} = \frac{C(s)P(s)}{1+C(s)P(s)} = \frac{K_D s+K_P}{ts^2+(1+K_D)s+K_P} \tag{6}$$

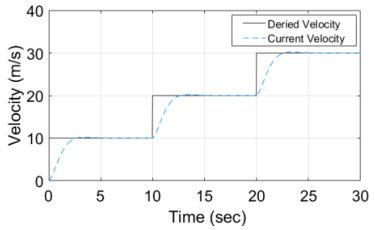

Figure 4. Simulation result for longitudinal PD control.

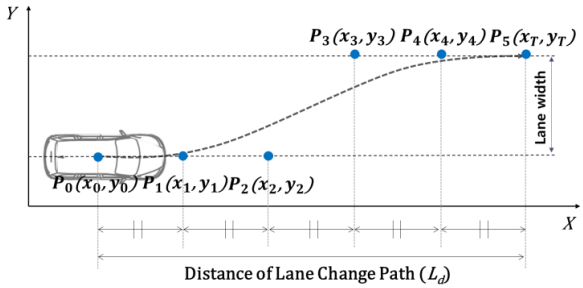

Figure 5. Quintic Bezier curve generation for LCM.

where V_{des} represents the desired velocity and V_x is the current longitudinal velocity of the vehicle. Fig. 3 represents the block diagram of the feedback system with a plant model, P(s) with $K_P = 1$, $K_D = 0.1$, and $t = 0.5$. Fig. 4 shows the simulation result for the longitudinal PD controller.

III. Lane Change Maneuver

A. Quintic Bezier Curve

Lane change maneuver is performed using a virtual trajectory that is not directly measured. There are various techniques used for generating continuous curvature paths; Bezier curve is one of the typical curve generation algorithms used in many applications [17]. We adopted Bezier curve because the curvature of the generated path can easily be managed by placing the control points. When the degree of the Bezier curve is 5, the curve is defined as follows [17-18],

$$f_{x,y} = \sum_{i=0}^{5} \binom{5}{i} (1-\tau)^{5-i} \tau^i P_{x_i,y_i} \quad (0 \le \tau \le 1) \qquad (7)$$

where $f_{x,y}$ and P_{x_i,y_i} are the coordinates of the Bezier curve points and the position of each control point in 2-dimensional coordinates. In this study, each control point, P_i (x_i, y_i) are put with regular intervals within a lane change distance, L_d for simplicity of the curvature-related variables of the Bezier curve. In this study, P_0 and P_5 are determined by the current location of the vehicle and the target position at a lane change distance considering a lane width, as shown in Fig. 5.

B. Lane Change Algorithm

If lane change or obstacle avoidance is required while driving the route in the map, a local path needs to be generated in real time. In this case, considering the current driving speed of the vehicle, a path that satisfies the limit range of the lateral acceleration is dynamically generated in the trajectory planning stage in real time.

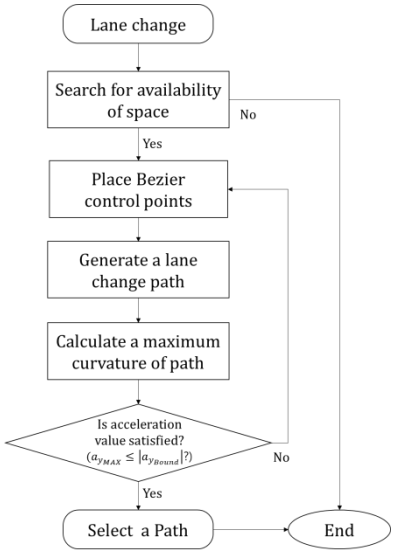

Figure 6. Flow chart for the proposed lane change path generation algorithm.

In the proposed algorithm, the curvature of the generated Bezier curve is evaluated by user input parameter of lateral acceleration values to limit the lateral motion. Fig. 6 describes the LCM path generation algorithm that concurrently satisfies the lateral acceleration. If a lane change maneuvering is required, space availability needs to be confirmed first for local path generation. In the next step, the trajectory planning block generates possible paths, and the generated local path is evaluated to ascertain whether it meets the given acceleration constraint.

Once the vehicle selects a generated local path, the following acceleration must be satisfied,

$$a_{y_{MAX}} \le |a_{y_{Bound}}| \qquad (8)$$

where $a_{y_{MAX}}$ denotes the maximum kinematic lateral acceleration of the Bezier curve, and $a_{y_{Bound}}$ is the user lateral acceleration parameter value for the LCM. The kinematic maximum acceleration from a curvature can be calculated using the following equations:

$$a_{y_{MAX}} = {V_x}^2 \cdot k_{Bezier} \qquad (9)$$

Here, V_x denotes the longitudinal speed of the vehicle, and k_{Bezier} denotes the maximum curvature of the Bezier curve. To obtain a maximum curvature, we perform a linear interpolation of the 1-D points array of the Bezier curve points. In this study, we set $N = 100$ as an empirical parameter.

$$k_{Bezier} = max \begin{bmatrix} |k_1| \\ \vdots \\ |k_N| \end{bmatrix}_{N \times 1} \qquad (10)$$

$$k = \frac{y''}{\left(1+y'^2\right)^{\frac{3}{2}}} \left(y' = \frac{dy}{dx}, y'' = \frac{d^2y}{dx^2}\right)$$

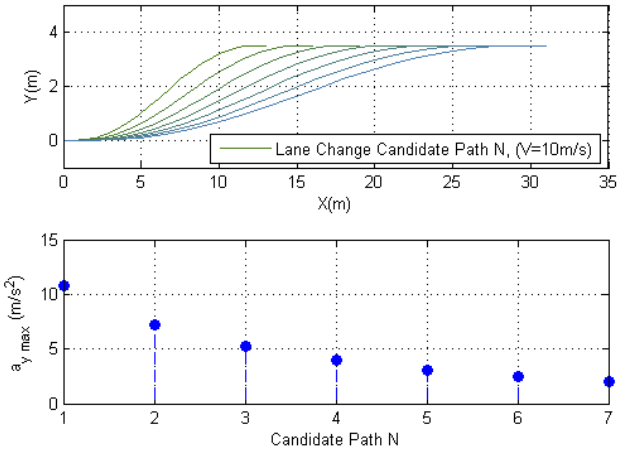

Figure 7. Elicited results for LCM path evaluation.

If the kinematic lateral acceleration at the point of maximum curvature of the curve with respect to the current velocity is less than the predefined lateral acceleration, $|a_{y_{Bound}}|$, it can be satisfied throughout the generated paths. If the condition in Eq. (8) is not satisfied, then the local path planner regenerates a new path by placing a set of P3, P4, and P5 at a distance far away from the current location of the vehicle. In this study, the distance interval was set to 5 meters to generate the next candidate path.

Fig. 7 shows the simulated results for the path evaluation and the selection process used to validate the proposed path generation algorithm when the given acceleration magnitude is 2.0 m/s^2 maintaining a 10 m/s speed. As seen from Fig. 6, point P_5 was moved far away in the generated path under the evaluation process. This evaluation was iterated until the condition in Eq. (8) was satisfied. In the calculated results shown in Fig. 6, the 7th path satisfies the criterion, and it is thus selected as the lane change desired path.

IV. Simulations

A. Simulation Environment

The proposed LCM was tested using Simulink-CarSim (Fig. 8). CarSim is well known as an accurate tool for simulating vehicle dynamic motion in the automotive industry [19]. The vehicle model parameters are presented in TABLE I. The E-class model, which is provided as a default vehicle model, was used. The mass and the wheelbase for this vehicle are respectively 1,740 kg and 3.05 meters. The vehicle dynamic simulation based on the proposed controller and LCM algorithm was conducted at different constant speeds.

TABLE I. Vehicle Model Parameters

Parameters	Notation	Value
Vehicle mass	m	1,740 kg
Vehicle yaw moment	I_z	3000 kgm^2
Front-c.g. distance	l_f	1.4 m
Rear-c.g. distance	l_r	1.65 m
Cornering stiffness of front tires	C_{af}	81000 N/deg
Cornering stiffness of rear tires	C_{ar}	81000 N/deg

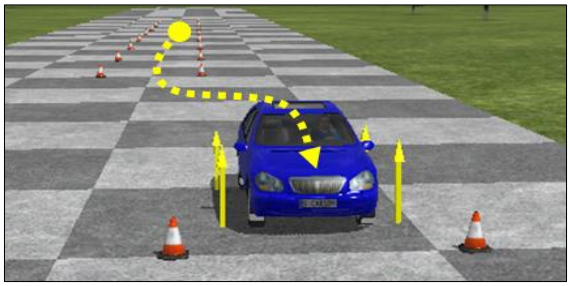

Figure 8. Snapshot of Simulink-CarSim during LCM.

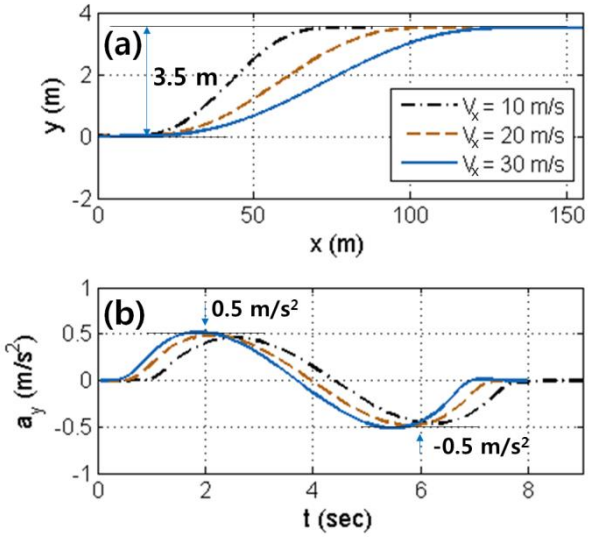

Figure 9. Lane-change maneuvers performed by Simulink-CarSim (a) trajectories of the lane change, and (b) simulated lateral accelerations of the vehicle.

TABLE II. Results of Number of Iteration for Generating a Suitable LCM Path and Computation Time

V_x (m/s)	Number of iterations	Computation Time (ms)
10	13	218
20	26	267
30	39	322

B. Simulation Results

The results of the lane change maneuvering and path following are presented in Fig. 9 for given lateral acceleration criteria is expressed by $|a_{y_{Bound}}| = 0.5$ m/s^2. Fig. 9 (a) shows the lane change trajectories driven by the simulated vehicle and (b) the lateral acceleration during lane changes. As shown in Fig. 9 (b), the vehicle lateral acceleration shows trends saturated up to the given lateral acceleration value despite various speed conditions from 10 m/s to 30 m/s.

TABLE II shows the number of iterations and computation time to measure the real-time performance. For the test, a desktop computer with Intel Core i5-6200 CPU and 8GB RAM was used. The number of iterations and cost increases as the vehicle speed increases, however, the entire path generation algorithm was completed within about 218 to 322 ms in each case.

Figure 10. Photo of the autonomous vehicle used for the real road experiment.

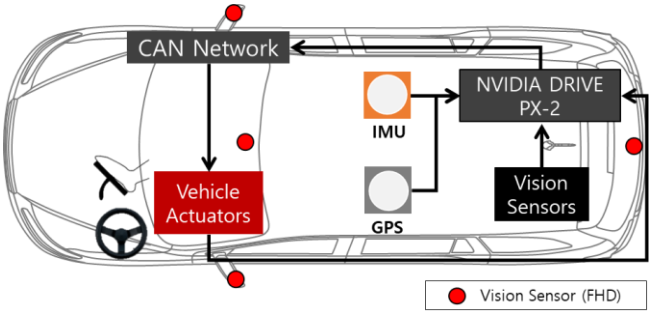

Figure 11. Hardware structure of the autonomous vehicle equipped with the proposed control system.

V. Experiments

A. On-vehicle Hardware System

For the real-road experimental test of the proposed controller and LCM algorithm, we used a modified autonomous commercial vehicle equipped with sensors and actuators, as shown in Fig. 10 and Fig. 11. Despite the compactness of the car, the test vehicle (RAY from Kia motors) provides enough space for on-vehicle sensors. This vehicle has a gasoline-powered engine, front wheel drive and motor-driven power steering (MDPS). In addition, it has permission for autonomous driving from the Ministry of Land, Infrastructure and Transport of South Korea.

To implement the proposed controller, we developed a control system structure (Fig. 11) using NVIDIA Drive PX-2 as a main controller. It has enough computing power to perform the proposed path planning and vehicle control algorithms. In addition, it is mainly used for image processing to extract lane markers on the road and obstacles in the vehicle's surrounding with the front vision and surround view cameras based on DNN perception engines [23].

A GPS antenna was mounted on the roof of the vehicle considering the center of the car rear axle, and an IMU sensor was installed in the truck space at the same geometrical position as the GPS antenna. We used MRP-2000 GPS sensors, which can support the Network-RTK to achieve high performance in position accuracy, with a position error tolerance of within ±2 cm. In addition, an IG-500A IMU sensor was used to measure the dynamic motion of the vehicle, including the yaw angle, lateral acceleration, longitudinal acceleration, etc. All the data from the vehicle-mounted sensors were synchronized to 10 Hz.

B. Results of the Lane Change Maneuver

The goal of the lane change experiment validates the lane change maneuvering that meets user input parameter of lateral acceleration bound maintaining the current speed. Lane change maneuvering was executed on a plain field with a 3.5-meter road width and conducted for different speeds at 10 m/s and 15 m/s, respectively, bounding $|a_{y_{Bound}}| = 1.0$ m/s^2 of the lateral acceleration limit. In this experiment, it is important that the peak lateral acceleration should be bounded even though at different speeds.

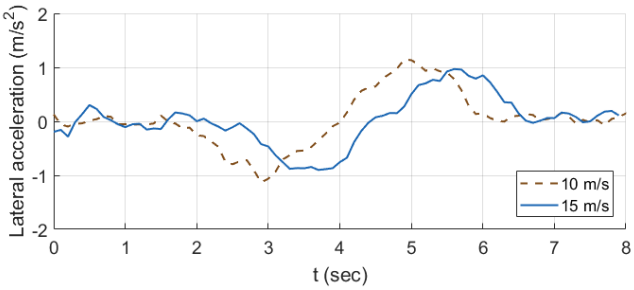

Figure 12. Measured IMU sensor data during lane-change maneuvers performed by the autonomous vehicle.

Fig. 12 illustrates the experimental results for the lane-change maneuvers performed by the autonomous vehicle. The tests were conducted under vehicle velocities of 15 m/s and 10 m/s, respectively. The results show that the maximum value of lateral acceleration for the vehicle is regulated below the criterion of the given lateral acceleration bound.

VI. Conclusion

In this work, we verified the performance of the proposed LCM method and vehicle controller through computer simulations and a real experiment. The proposed method can be applied at the local path planning stage to achieve smooth transition in lateral motion of vehicles during lane change maneuvering. Our future work will involve developing a method for the path planning in complex environments as well as considering personal lateral acceleration preferences for smoother and safer control even on sharp curved roads.

Acknowledgment

This research was supported by the MSIT (Ministry of Science and ICT), Korea, under the "ICT Consilience Creative Program" (IITP-2019-2017-0-01015) supervised by the IITP (Institute for Information & Communications Technology Planning & Evaluation). The authors performed this work as a part of research projects of SKT-Yonsei Cooperative Autonomous Driving Research Center under the SKT-Yonsei Global Talent Fostering Program supported by the SK Telecom ICT R&D Center.

REFERENCES

[1] M. Elbanhawi, M. Simic, and R. Jazar. "In the Passenger Seat: Investigating Ride Comfort Measures in Autonomous Cars," IEEE Intelligent Transportation Systems Magazine, vol. 7, no. 3, pp. 4-17, 2015.

[2] J. Eriksson, and L. Svensson, "Tuning for Ride Quality in Autonomous Vehicle: Application to Linear Quadratic Path Planning Algorithm," Dissertation, UPPSALA University, 2015.

[3] M. Elbanhawi, S. Milan, and J. Reza, "The Effect of Receding Horizon Pure Pursuit Control on Passenger Comfort in Autonomous Vehicles," Intelligent Interactive Multimedia Systems and Services 2016. Springer International Publishing, pp 335-345, 2016.

[4] I. Bae, J. Y. Moon, and S. Kim, "Self-Driving like a Human driver instead of a Robocar: Personalized comfortable driving experience for autonomous vehicles," 3rd International Conference on Electric Vehicle, Smart Grid and Information Technology, 2018.

[5] C. Diels, "Will autonomous vehicles make us sick," CRC Press, 2014

[6] M. Sivak, and S. Brandon, "Motion sickness in self-driving vehicles," The University of Michigan Transportation Research Institute, 1-13, 2015.

[7] SAE J3016, "Taxonomy and definitions for terms related to driving automation systems for on-road motor vehicles," 2016, available: http://cyberlaw.stanford.edu/files/blogimages/LevelsofDrivingAutomation.pdf

[8] D. Martin, and D. Litwhiler, "An Investigation of Acceleration and Jerk Profiles of Public Transportation Vehicles," presented at the American Society for Engineering Education, AC 2008-1330, 2008

[9] A. KILINÇ, and T. Baybura, "Determination of minimum horizontal curve radius used in the design of transportation structures, depending on the limit value of comfort criterion lateral jerk," TS06G-Engineering Surveying, Machine Control and Guidance, 2012.

[10] Choi, J. W., Curry, R., & Elkaim, G. "Path planning based on bézier curve for autonomous ground vehicles," In World Congress on Engineering and Computer Science 2008, WCECS'08., pp. 158-166, 2008.

[11] L. Han, H. Yashiro, T. N. Nejad, Q. H. Do and S. Mita, "Bezier curve based path planning for autonomous vehicle in urban environment," in *Proc. IEEE Intell. Veh. Symp. (IV)*, San Diego, CA, pp.1036-1042, 2010.

[12] J. Chen, P. Zhao, T. Mei, and H. Liang, "Lane change path planning based on piecewise Bezier curve for autonomous vehicle," IEEE International Conference on Vehicular Electronics and Safety, pp. 17-22, 2013.

[13] K. Kawabata, L. Ma, J. Xue, C. Zhu, and N. Zheng, "A path generation for automated vehicle based on Bezier curve and via-points," Robotics and Autonomous Systems, 74, pp. 243-252, 2015.

[14] N. Monot, X. Moreau, A. Benine-Neto, A. Rizzo, and F. Aioun, "Design of a Weighted Multi-Controller for Lateral Guidance of Autonomous Vehicles Using Steering Control," IEEE, 26th Mediterranean Conference on Control and Automation, pp. 1-7, 2018.

[15] R. Rajamani, "Vehicle dynamics and control," Springer, 2011.

[16] I. Bae, J. H. Kim and S. Kim, "Steering rate controller based on curvature of trajectory for autonomous driving vehicles," *IEEE Intelligent Vehicle Symposium (IV)*, Gold Coast, Australia, pp. 1381-1386, 2013.

[17] A. Ravankar, Y. Kobayashi, Y. Hoshino, and C. Peng, "Path smoothing techniques in robot navigation: State-of-the-art, current and future challenges," Sensors, 18(9), 2018.

[18] I. Bae, J. Y. Moon, H. B. Park and S. Kim, "Path generation and tracking based on a Bezier curve for a steering rate controller of autonomous vehicles," IEEE International Conference on Intelligent Transportation Systems (ITSC), pp. 436-441, 2013.

[19] J. M. Snider, "Automatic steering methods for autonomous automobile path tracking," *Robotic Institute, Carnegie Mellon Univ., Pittsburgh, PA, Tech. Rep.* CMU-RITR-09-08, 2009.

[20] R. Attia, O. Rodolfo, and B. Michel, "Combined longitudinal and lateral control for automated vehicle guidance," Vehicle System Dynamics 52(2), 261–279, 2014.

[21] P. Bosetti, L. Mauro, and S. Andrea, "On the human control of vehicles: an experimental study of acceleration," European Transport Research Review 6(2), 157–170, 2014.

[22] P. Bosetti, M. Da Lio and A. Saroldi, A, "On curve negotiation: from driver support to automation," IEEE Transactions on Intelligent Transportation Systems, 16(4), pp.2082-2093, 2015.

[23] J. Jung, I. Bae, J. Moon, T. Kim, J. Kim and S. Kim, "End-to-End Steering Controller with CNN-based Closed-loop Feedback for Autonomous Vehicles", *IEEE Intelligent Vehicle Symposium (IV)*, Changshu, China, pp. 617-622, 2018.